J. Fluid Mech. (1971), *vol.* 47, *part* 3, *pp.* 449–468
Printed in Great Britain

Response behaviour of hot wires in shear flow

By F. B. GESSNER AND G. L. MOLLER
Department of Mechanical Engineering, University of Washington

(Received 2 July 1970 and in revised form 28 October 1970)

The response characteristics of a hot wire operated at constant temperature and exposed to a mean-velocity gradient along its length are examined both analytically and experimentally. The shear sensitivity of local wire temperature distributions, as measured with an infrared microscope, are compared with predicted temperature distributions in order to select a convective heat transfer correlation which can be applied locally along a wire in shear flow. On the basis of this correlation, the steady-state and dynamic response behaviour of platinum and tungsten wires in shear flow are examined by means of computer-generated data. Response curves of general applicability are presented which can be used to correct local mean-velocity and turbulence intensity measurements whenever a mean-velocity gradient exists along a wire.

1. Introduction

Previous work has centred on the response characteristics of hot wires in a uniform mean flow as a function of Reynolds number, Mach number, overheat ratio, sensitivity to yaw, and wire length-to-diameter ratio. Champagne, Sleicher & Wehrmann (1967), as well as Friehe & Schwarz (1968), present summaries of work that has been done on steady-state response behaviour in uniform incompressible flow. Both references also discuss procedures for correcting Reynolds stress measurements with inclined wires when the convective heat loss is altered by tangential cooling effects. The present state of knowledge with respect to dynamic response behaviour in a uniform flow is well summarized by both Corrsin (1963) and Hinze (1959, chapter 2).

In contrast, very little work has been done in examining the response behaviour of hot wires exposed to a non-uniform mean flow. Specifically, the analyses of Mattioli (1956) and Furth (1956), as discussed by Corrsin (1963), were the only pertinent references found in the literature. The results of their analyses indicate that the presence of a mean-velocity gradient along a wire alters the local wire temperature distribution. Neither Furth nor Mattioli, however, examined the influence of a non-uniform mean flow on wire calibration, i.e. convective heat loss behaviour, or dynamic response behaviour.

The present study was undertaken, therefore, in order to investigate in some detail the response behaviour of hot wires when exposed to a mean shear. As an initial effort, hot wires normal to the mean-flow direction in the presence of a linear mean-velocity gradient are considered herein. For purposes of examining the effect of a linear mean shear, it is expedient to define a shear parameter S

as $(\Delta\overline{U}/\overline{U}_c)/(l/d)$, where $\Delta\overline{U}$ is the mean-velocity increment across the wire, $\overline{U}_c$ is the mean velocity at the wire centreline, and l/d is the length-to-diameter ratio of the wire (refer to figure 1). The above definition for S can be rationalized by first noting that any shear parameter formulation must depend on $\partial\overline{U}/\partial z$ or, equivalently, $\Delta\overline{U}/l$ since $\Delta\overline{U}/l = \partial\overline{U}/\partial z$. In order to define a dimensionless shear parameter, it is necessary to select both length and velocity scales which can be used to normalize $\Delta\overline{U}/l$. With reference to figure 1, these scales are most suitably chosen as d and $\overline{U}_c$, respectively. Although it may not be physically obvious that

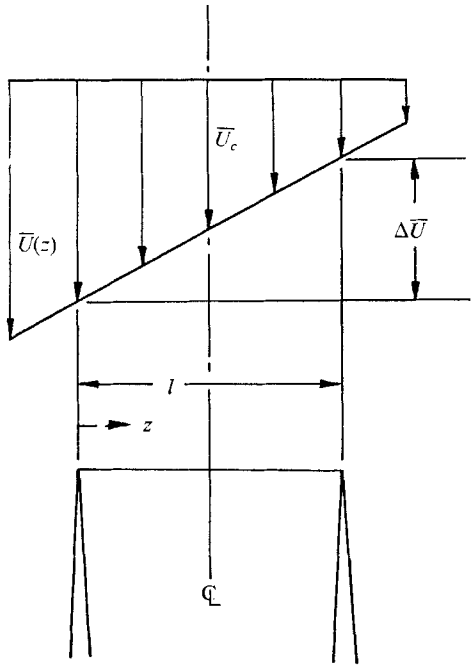

FIGURE 1. Shear parameter formulation: $S \equiv (\Delta\overline{U}/\overline{U}_c)/(l/d)$.

d is associated with mean-shearing effects, this variable does influence the response characteristics of a wire exposed to a mean shear. This can be demonstrated by noting that results for overall response behaviour depend ultimately on the solution to either a steady-state or time-dependent wire energy balance, both of which contain terms involving d^2 and d^4 (refer to equations (1) and (7)).

On the basis of the above shear parameter formulation, S is invariant for wires of a given diameter but of different length exposed to a given mean-velocity gradient with a specified mean velocity at the wire centre. This means that the relative influence of a mean shear on the response characteristics of wires of fixed diameter but of different length can be examined by comparing results for different l/d wires at the same value of S.

The influence of S on wire response behaviour will be examined in subsequent discussion for different specifications of wire material, length-to-diameter

ratio, and overheat ratio. In the present study the overheat ratio is defined as $\mathscr{H} = (\bar{R}_{w,m} - R_\infty)/R_\infty$, where R_∞ is the wire resistance at the ambient temperature and $\bar{R}_{w,m}$ is the resistance of the wire evaluated at the overall mean temperature of the wire under heated conditions.

2. Analytical considerations

2.1. *Steady-state response analysis*

In order to examine the influence of a mean-velocity gradient on the steady-state response of a hot wire, it is first necessary to determine the influence of the gradient on the local wire temperature distribution, which, in turn, affects its convective heat loss characteristics. An energy balance applied to an internally heated, finite-length wire includes several energy transfer mechanisms. In general, the various mechanisms are: (i) internal heat generation, (ii) axial heat conduction, (iii) radial heat conduction, (iv) energy transfer between the wire and the surrounding fluid by means of forced convection, (v) free convection, (vi) radiation, and (vii) energy losses resulting from a thermoelectric effect at the wire–probe support junctions.

On the basis of measurements by Van der Hegge Zijnen (1956), Hinze suggests that free convection can be neglected when $Re_f > 0{\cdot}5$ and $Gr_f Pr_f < 10^{-4}$, where Re_f, Gr_f, and Pr_f are the Reynolds number, Grashof number, and Prandtl number with fluid properties evaluated at the mean film temperature, T_f, with $T_f \equiv \frac{1}{2}(\bar{T}_w + T_\infty)$, where $\bar{T}_w$ = local mean wire temperature and T_∞ = ambient temperature. The latter condition was satisfied locally along a wire over the range of variables considered herein, so free convection effects were neglected in the analysis. Also neglected were radiation losses, which were estimated to be at least two orders of magnitude smaller than losses by forced convection. Possible energy dissipation because of thermoelectric effects was also estimated to be small on the basis of comments by Davies & Fisher (1964). Finally, for the l/d ratios considered herein ($l/d \geqslant 200$) radial heat conduction effects were neglected without reservation.

In accordance with the above considerations, a steady-state energy balance applied to an elemental wire length yields the following differential equation:

$$a^2 \frac{d}{dz}\left(k_w \frac{d\bar{T}_w}{dz}\right) + \bar{I}^2 \rho_w - pa\bar{h}(\bar{T}_w - T_\infty) = 0, \tag{1}$$

where $\bar{I}$ = wire current; $k_w = k_w(\bar{T}_w)$, the local wire thermal conductivity; $\rho_w = \rho_w(\bar{T}_w)$, the local wire resistivity; p = wire perimeter; $a = \frac{1}{4}\pi d^2$, the wire cross-sectional area; $\bar{h} = \bar{h}(\bar{T}_w, \bar{U})$, the local convective heat transfer coefficient.

The dependency of k_w and ρ_w on $\bar{T}_w$ over the temperature range of interest in this study ($20\,^\circ\mathrm{C} \leqslant \bar{T}_w \leqslant 400\,^\circ\mathrm{C}$) can be written as

$$\left.\begin{aligned} k_w &= k_{w0}(1 + \beta \bar{T}_w), \\ \rho_w &= \rho_{w0}(1 + \zeta_1 \bar{T}_w + \zeta_2 \bar{T}_w^2), \end{aligned}\right\} \tag{2}$$

where k_{w0} and ρ_{w0} are reference values and β, ζ_1, and ζ_2 are the temperature coefficients. The values utilized in the analysis for both platinum and tungsten wire materials are given by Moller (1969).

In order to develop an expression for the convective heat transfer coefficient as a function of local mean velocity and wire temperature, correlations developed for uniform flow over a wire at uniform temperature were applied locally along a wire. Because Mach number and Knudsen number effects are negligible over the range of conditions specified herein, two empirical correlations developed by Kramers (1946) and Collis & Williams (1959) for incompressible flow were utilized. Both relationships can be written in the following generalized form:

$$Nu_f = (A + BRe_f^n)(T_f/T_\infty)^{\alpha_1}, \tag{3}$$

where $Nu_f = \bar{h}d/k_f$, the Nusselt number; $Re_f = \bar{U}d/\nu_f$, the Reynolds number; A, B, n, and α_1 are numerical constants (provided the Prandtl number is constant in Kramers' correlation) and assume different values for each correlation. Since these correlations were first proposed, Kjellström & Hedberg (1968) and Davies & Bruun (1968) have developed alternate empirical correlations which they feel more accurately describe the convective heat loss behaviour of heated wires. None of these investigators, however, develop correlations in dimensionless form which apply over a wide range of operating conditions, so only (3) was applied in the present work.

The dependency of k_f and ν_f on local wire temperature was evaluated from $k_f = k_\infty(T_f/T_\infty)^{\alpha_2}$, $\nu_f = \nu_\infty(T_f/T_\infty)^{\alpha_3}$, with $\alpha_2 = 0{\cdot}836$ and $\alpha_3 = 1{\cdot}714$, for air over the range of values of T_∞ and T_w considered herein. Both expressions were expanded in series form by introducing a normalized temperature difference $\Theta = (\bar{T}_w - T_\infty)/T_\infty$. For platinum and tungsten wires operating at $\mathscr{H} \leqslant 0{\cdot}8$, the following generalized form was developed:

$$\bar{h}(\Theta, \bar{U}) = \frac{Ak_\infty}{d}(1 + \xi_1\Theta + \xi_2\Theta^2) + \frac{Bk_\infty d^{n-1}}{\nu_\infty^n}(1 + \gamma_1\Theta + \gamma_2\Theta^2)\bar{U}^n, \tag{4}$$

with

$$\begin{aligned}
\xi_1 &= \tfrac{1}{2}(\alpha_1 + \alpha_2),\\
\xi_2 &= \tfrac{1}{8}(\alpha_1 + \alpha_2)(\alpha_1 - \alpha_2 - 1),\\
\gamma_1 &= \tfrac{1}{2}(\alpha_1 + \alpha_2 - \alpha_3 n),\\
\gamma_2 &= \tfrac{1}{8}(\alpha_1 + \alpha_2 - \alpha_3 n)(\alpha_1 + \alpha_2 - \alpha_3 n - 1).
\end{aligned}$$

If the expressions given by (2) and (4) are substituted into (1), and if $\eta \equiv z/l$, a normalized differential equation for the wire temperature distribution can be written as

$$(C_1 + C_2\Theta)\,d^2\Theta/d\eta^2 + C_2(d\Theta/d\eta)^2 + F_1(\eta)\,\Theta^3 + F_2(\eta)\,\Theta^2 + F_3(\eta)\,\Theta + C_3 = 0, \tag{5}$$

with

$$\begin{aligned}
C_1 &= \frac{a^2 k_{w0} T_\infty}{l^2}(1 + \beta T_\infty),\\
C_2 &= \frac{a^2 k_{w0} T_\infty^2 \beta}{l^2},\\
C_3 &= \bar{I}^2 \rho_{w0}(1 + \zeta_1 T_\infty + \zeta_2 T_\infty^2),\\
F_1(\eta) &= -\frac{pak_\infty T_\infty}{d}\left[A\xi_2 + B\gamma_2\left(\frac{\bar{U}d}{\nu_\infty}\right)^n\right],
\end{aligned}$$

$$F_2(\eta) = \bar{I}^2 T_\infty^2 \rho_{w0} \zeta_2 - \frac{pak_\infty T_\infty}{d}\left[A\xi_1 + B\gamma_1 \left(\frac{\bar{U}d}{\nu_\infty}\right)^n\right],$$

$$F_3(\eta) = \bar{I}^2 T_\infty \rho_{w0} (\zeta_1 + 2T_\infty \zeta_2) - \frac{pak_\infty T_\infty}{d}\left[A + B\left(\frac{\bar{U}d}{\nu_\infty}\right)^n\right],$$

where, in reference to figure 1, for a linear mean-velocity gradient

$$\bar{U} = \bar{U}_c[1 + (\Delta\bar{U}/\bar{U}_c)(\tfrac{1}{2} - \eta)]. \tag{6}$$

The boundary conditions that apply to (5) are that $\Theta = (\bar{T}_s - T_\infty)/T_\infty$ at $\eta = 0$ and $\eta = L$, where $\bar{T}_s$ is the wire temperature at each wire–probe support junction, which, in general, is not equal to T_∞ unless $d_s/d \gg 1$, where d_s is the probe support diameter. Initially, an attempt was made to solve (5) subject to the boundary conditions by means of a fourth-order Runge–Kutta technique. The solution diverged, however, regardless of the manner in which an initial assumed temperature gradient at one probe support was incremented and although the step-size was reduced to 0·1 % of the wire length. As an alternate approach, (5) was written in first central finite-difference form and solved successfully by means of an iterative technique using matrix inversion. Details of the numerical computations are given by Moller (1969).

2.2. *Dynamic response analysis*

The influence of thermal lag and non-uniform wire temperature on the dynamic response behaviour of a hot wire in shear flow can be examined by analyzing a time-dependent energy balance applied to the wire, namely

$$a^2 \frac{\partial}{\partial z}(k_w \partial T_w/\partial z) + I^2\rho_w - pah(T_w - T_\infty) = \tilde{\rho}_w c_w a^2 \partial T_w/\partial\theta, \tag{7}$$

where $\tilde{\rho}_w$ = wire mass density; c_w = wire specific heat; θ = time; and h, T_w, I and ρ_w are instantaneous values.

An expression for h in terms of the other variables can be developed by applying (3) locally along the wire. The justification for this procedure has been discussed by Corrsin (1963). For reasons to be given later, only Kramers' correlation will be utilized in the present development. Consider now constant-temperature operation for which $U = \bar{U}(z) + u'(z,\theta)$; $T_w = \bar{T}_w(z) + t'_w(z,\theta)$; $\rho_w = \bar{\rho}_w(z) + \rho'_w(z,\theta)$; and $I = \bar{I} + i'(\theta)$. Assume further that velocity fluctuations are small so that second-order effects can be neglected. If the above conditions are applied to (7), and the resulting equation is integrated over wire length, it follows that

$$\begin{aligned}\bar{I}^2 \int_0^l \rho'_w dz + 2\bar{I}i' \int_0^l \bar{\rho}_w dz = {} & \int_0^l [A + B(\bar{U}d/\nu_f)^n]\,\psi_f \rho'_w dz \\ & + Bn\int_0^l \psi_f (d/\nu_f)^n (\bar{\rho}_w - \rho_{w\infty})\,\bar{U}^{n-1} u' dz \\ & + \frac{a^2}{\rho_{w0}\zeta_1}\frac{\partial}{\partial\theta}\int_0^l \tilde{\rho}_w c_w \rho'_w dz - \frac{a^2}{\rho_{w0}\zeta_1}\frac{\partial}{\partial z}\int_0^l k_w \frac{\partial\rho'_w}{\partial z} dz,\end{aligned} \tag{8}$$

where $\psi_f \equiv pak_f/\rho_{w0}\zeta_1 d$.

In order to proceed with the integration, it is necessary either to know $\rho'_w(z)$ or assume that ρ'_w is uniform along the wire. The latter assumption will, of necessity, be applied now, although it is only an approximation. Further simplifications can be applied if it is noted that the temperature dependency of ψ_f/ν_f^n is rather weak. It is permissible, therefore, to let $\psi_f/\nu_f^n = \psi_{f,m}/\nu_{f,m}^n$, where the subscript m denotes quantities referred to the overall mean wire temperature, $\bar{T}_{w,m}$. For the moderate mean wire temperature variations associated with the present work, the first integral term on the right-hand side of (8) can be written as

$$\int_0^l A\psi_f \rho'_w dz = \frac{\rho'_w Apa}{\rho_{w0}\zeta_1 d}\int_0^l k_f\, dz \simeq \frac{\rho'_w Apalk_{f,m}}{\rho_{w0}\zeta_1 d}, \tag{9}$$

where exact equivalency applies if second-order effects are neglected. Finally, $\tilde{\rho}_w$ and c_w are essentially constant for both platinum and tungsten wires over the temperature range of interest ($20°\,\mathrm{C} \leqslant \bar{T}_w \leqslant 400\,°\mathrm{C}$). On the basis of these assumptions (8) simplifies to the following form:

$$\bar{I}^2\rho'_w l + 2\bar{I}i'\,a\bar{R}_{w,m} = A\psi_{f,m}\rho'_w l + B\psi_{f,m}\rho'_w\left(\frac{d}{\nu_{f,m}}\right)^n\int_0^l \bar{U}^n dz$$
$$+ Bn\psi_{f,m}\left(\frac{d}{\nu_{f,m}}\right)^n u'\int_0^l(\bar{\rho}_w - \rho_{w\infty})\bar{U}^{n-1}dz + \frac{\tilde{\rho}_w c_w a^2 l}{\rho_{w0}\zeta_1}\frac{d\rho'_w}{d\theta}, \tag{10}$$

where, on the basis of (6) and the binomial expansion,

$$\int_0^l \bar{U}^n dz \simeq \bar{U}_c^n l[1 + f_1(n)(\Delta\bar{U}/2\bar{U}_c)^2 + f_2(n)(\Delta\bar{U}/2\bar{U}_c)^4 + O(\Delta\bar{U}/2\bar{U}_c)^6], \tag{11}$$

with

$$f_1(n) = n(n-1)/3!,$$
$$f_2(n) = n(n-1)(n-2)(n-3)/5!,$$

where $f_1 = -1/24$ and $f_2 = -1/128$ for Kramers' correlation with $n = 0{\cdot}5$. Since $0 \leqslant \Delta\bar{U}/2\bar{U}_c < 1$, and the numerical coefficients of the higher-order terms decrease rapidly, terms of $O[(\Delta\bar{U}/2\bar{U}_c)^6]$ and higher can be neglected in (11).

In reference to (10), the resistivity fluctuation, ρ'_w, corresponds to a resistance fluctuation across the wire, r'_w, i.e. $\rho'_w = r'_w a/l$, and r'_w, in turn, is related to the current fluctuation, i', as follows: $i' = -g_{tr}\bar{I}r'_w$, where g_{tr} is the transconductance of the amplifier circuit of the anemometer (Hinze 1959). By means of the above relationships, (10) can be written as

$$\frac{di'}{d\theta} + \frac{\rho_{w0}\zeta_1}{\tilde{\rho}_w c_w a^2}\left\{\left[A + B\left(\frac{\bar{U}_c d}{\nu_{f,m}}\right)^n\right]\psi_{f,m}\left[1 + f_1(n)\left(\frac{\Delta\bar{U}}{2\bar{U}_c}\right)^2 + f_2(n)\left(\frac{\Delta\bar{U}}{2\bar{U}_c}\right)^4\right]\right.$$
$$\left. - \bar{I}^2 + 2\bar{I}^2\bar{R}_{w,m}g_{tr}\right\} i' = \frac{\rho_{w0}\zeta_1 g_{tr}\bar{I}Bn\psi_{f,m}}{\tilde{\rho}_w c_w a^3}\left(\frac{d}{\nu_{f,m}}\right)^n u'\int_0^l(\bar{\rho}_w - \rho_{w\infty})\bar{U}^{n-1}dz. \tag{12}$$

Equation (12) is of the form

$$\frac{di'}{d\theta} + \frac{i'}{M} = \phi(\theta), \tag{13}$$

where M can be characterized as the time constant of the hot-wire probe–anemometer system. If $Re_f \equiv \overline{U}_c d/\nu_{f,m}$, and if it is noted that $\psi_{f,m} = \pi a k_{f,m}/\rho_{w0}\zeta_1$, then M can be expressed as

$$M = \frac{\tilde{\rho}_w c_w a^2}{\pi a k_{f,m}(A + B\overline{Re}_f^n)\,[1 + f_1(n)\,(Sl/2d)^2 + f_2(n)\,(Sl/2d)^4] - \rho_{w0}\zeta_1(\bar{I}^2 - 2\bar{I}^2\bar{R}_{w,m}g_{tr})}. \tag{14}$$

On the basis of results to be discussed shortly, $\bar{I}$ decreases monotonically as S increases for constant-temperature operation at a fixed value of $\overline{Re}_f$. Since $g_{tr} \sim O(1/\bar{R}_{w,m})$, or larger, and $f_1(n)$ and $f_2(n)$ are negative coefficients, an increase in S causes both terms in the denominator of (14) to become smaller and, in turn, M to become larger. This, of course, has an undesirable effect on M, which, on the basis of (13), should be as small as possible to minimize thermal inertia effects. The relative influence of S on M for constant-temperature operation will be discussed in more detail later.

3. Experimental technique

The behaviour of a hot wire in shear flow was examined experimentally by taking wire temperature profile measurements in a free-turbulent circular jet in the region where similar velocity profiles prevail. In the central portion of the jet ($0{\cdot}5 \leqslant r/r^* \leqslant 1{\cdot}5$, where r is radial distance from the jet centreline and r^* is the value of r at which $\overline{U}$ is one-half the centreline velocity), axial mean-velocity profiles were essentially linear. By selectively locating a hot wire at points along a line of constant axial mean velocity downstream of the jet exit, it was possible to take measurements with the free-stream Reynolds number constant ($\overline{Re}_\infty = \overline{U}_c d/\nu_\infty$) while varying the shear parameter, S, in a systematic manner.

A Pitot tube whose axial and radial positions in the jet could be determined to within $\pm 0{\cdot}01$ and $\pm 0{\cdot}001$ in., respectively, was used in conjunction with an inclined manometer to measure mean-velocity profiles. All hot-wire measurements in the jet were made at $T_\infty = 30 \pm 0{\cdot}5$ °C with 0·001 in. diameter wires for which $l/d \simeq 300$. Sigmund Cohn pure reference grade platinum wire was used, and the hot wires were mounted on music wire supports in a manner suggested by Champagne (1966). The wire supports were 0·025 in. in diameter and tapered at the end with $d_s/d \simeq 10$ at the wire-support junctions. Each wire was operated on a constant-temperature basis by means of a Thermo-systems Model 1010 Anemometer. Local wire temperature distributions were measured by means of a Barnes Engineering RM-2A infrared microscope with an electronic control unit whose voltage output was read out on a digital voltmeter.

In order to correlate the output of the microscope with local wire temperature, a calibration procedure using platinum foil was applied initially (Champagne 1966). This technique yielded unsatisfactory results, however, because free convection from the platinum foil caused the response of the microscope to be unstable and non-reproducible. As an alternate approach, a 0·001 in. diameter platinum wire with $l/d = 2500$ was fabricated, and the central portion of the wire was scanned with the microscope for several operating values of overheat ratio.

This procedure yielded a calibration curve interrelating microscope response with wire centreline temperature, $\overline{T}_{w,c}$, assuming that $\overline{T}_{w,c} \simeq \overline{T}_{w,m}$. The calibration curve tended to underestimate, therefore, the local wire temperature for a given voltage output from the microscope. In order to correct this curve, the wire was scanned with the microscope along its entire length for several values of $\overline{T}_{w,m}$. The calibration curve was then used to evaluate local wire temperature distributions, and the percentage deviation of $\overline{T}_{w,c}$ from $\overline{T}_{w,m}$ at each overheat ratio was determined by means of a planimeter. This same percentage deviation (~ 2 to 3%) was applied to the original calibration curve in order to correct the initial deficiencies in the curve.

By calibrating in the above manner, it was not necessary to correct the calibration curve for differences in ambient surroundings between calibrating and operating conditions (Champagne 1966). Furthermore, by calibrating with a wire instead of foil, it was not necessary for the wire to fill completely the spot size of the objective lens. This meant that measurements could be made at a relatively large focal length to minimize possible interference effects between the microscope lens and the flow field.

4. Results and discussion

4.1. *Temperature distributions*

The influence of a mean-velocity gradient on the local measured temperature distribution along a wire under typical operating conditions is shown in figure 2. For all cases the overheat ratio calculated by integrating each temperature profile ($0{\cdot}777 \leqslant \mathscr{H} \leqslant 0{\cdot}798$) agreed favourably with $\mathscr{H} = 0{\cdot}8$, as set on the anemometer. The figure indicates that an increase in the mean-velocity gradient along a wire causes an increase in the skewness of its local temperature distribution. The wire end support temperatures, however, are essentially independent of S for $0 \leqslant S \leqslant 3 \times 10^{-3}$ and, on the basis of additional data, also $\overline{Re}_\infty$ for $6{\cdot}82 \leqslant \overline{Re}_\infty \leqslant 21{\cdot}4$. Over the range of values of S and $\overline{Re}_\infty$ mentioned above, $\overline{T}_s = 60 \pm 3\,^\circ\mathrm{C}$ and $86 \pm 3\,^\circ\mathrm{C}$ for $\mathscr{H} = 0{\cdot}4$ and $0{\cdot}8$, respectively. These temperature values are based on extrapolated data since the measured wire temperatures at the end supports were excessively high, an effect also noted by Champagne (1966) in his experiments.

The applicability of Kramers' and Collis & Williams' correlations locally along a wire was examined by comparing experimentally measured temperature distributions with those predicted from the analysis. Typical results shown in figure 3 indicate excellent agreement between the measurements and predicted temperature distributions utilizing Kramers' correlation. The distributions based on Collis & Williams' correlation, however, deviate somewhat from the experimental data and also indicate abnormal temperature gradient behaviour at the end supports. These effects diminish for higher overheat ratios (figure 4) but the same discrepancies still exist.

In order to seek an explanation for this behaviour, temperature distributions based on Collis & Williams' correlation were generated from the computer

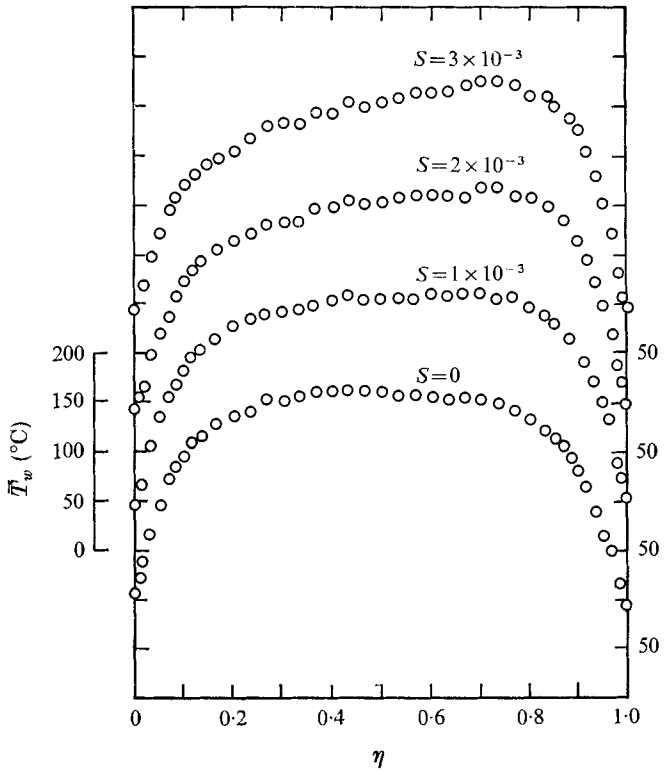

FIGURE 2. Influence of a mean-velocity gradient on wire temperature distributions: $l/d \simeq 300$, $\mathscr{H} \simeq 0{\cdot}8$, $\overline{Re}_\infty = 6{\cdot}82$.

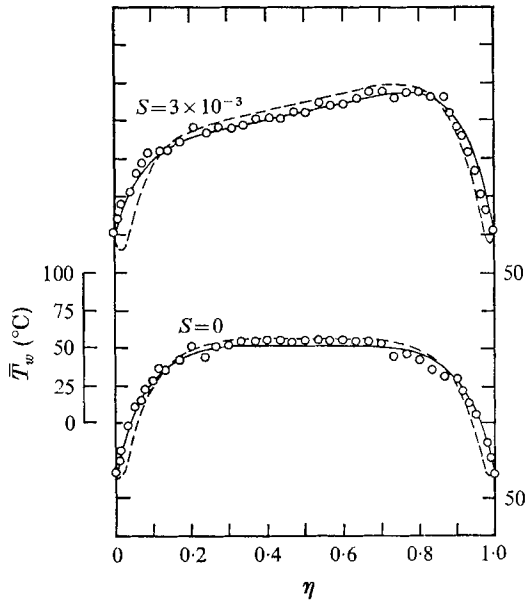

FIGURE 3. Comparison between analytical and experimental temperature distributions: $l/d \simeq 300$, $\mathscr{H} \simeq 0{\cdot}4$, $\overline{Re}_\infty = 6{\cdot}82$. – – –, Collis & Williams; ——, Kramers.

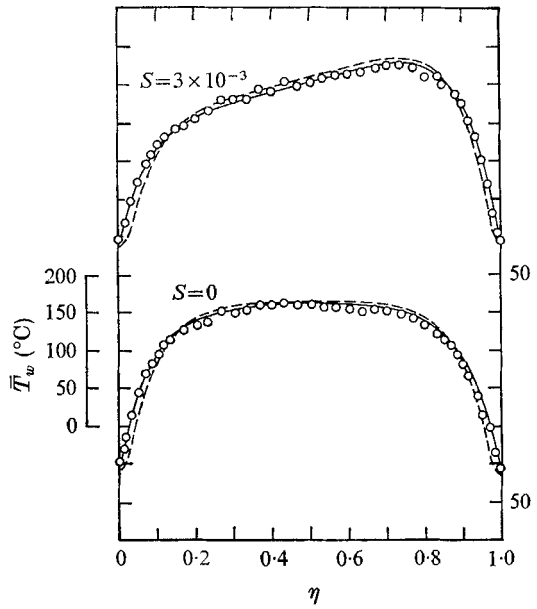

FIGURE 4. Comparison between analytical and experimental temperature distributions: $l/d \simeq 300$, $\mathscr{H} \simeq 0{\cdot}8$, $\overline{Re}_\infty = 6{\cdot}82$. – – –, Collis & Williams; ——, Kramers.

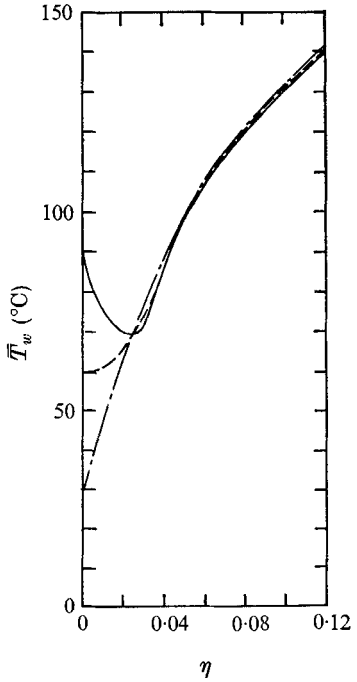

FIGURE 5. Effect of end support temperature variations on wire temperature distributions (Collis & Williams' correlation): $l/d \simeq 300$, $\mathscr{H} = 0{\cdot}4$, $\overline{Re}_\infty = 6.82$, $\bar{T}_\infty = 30\,°\mathrm{C}$, $S = 0$. $\bar{T}_s$ in °C: ——, 90; – – –, 60; — – —, 30.

program for $S = 0$ with $\overline{T}_s \geqslant T_\infty$. (Note that, in figures 2–4, $\overline{T}_s > T_\infty$ for all cases.) The results of these computations are shown in figure 5 and indicate that the local wire temperature distribution approaches normalcy as $\overline{T}_s$ approaches T_∞. For the condition when $\overline{T}_s = T_\infty$, additional computations showed that both Kramers' and Collis & Williams' calculations yield essentially the same temperature distributions over a range of values of $\mathscr{H}$, S, and $\overline{Re}_\infty$. Because further computations were contemplated with $\overline{T}_s \geqslant T_\infty$, however, all subsequent analytical results reported herein are based on Kramers' correlation.

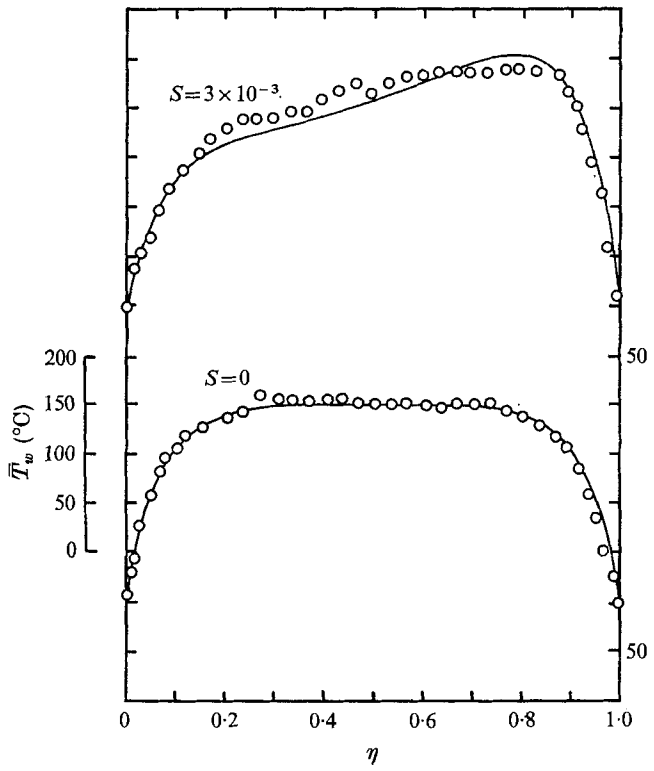

FIGURE 6. Influence of a mean-velocity gradient on wire temperature distributions (Kramers' correlation): $l/d \simeq 300$, $\mathscr{H} \simeq 0{\cdot}8$, $\overline{Re}_\infty = 21{\cdot}4$.

Figure 6 shows a comparison between theoretical and measured temperature distributions for a free-stream Reynolds number ($\overline{Re}_\infty = 21{\cdot}4$) greater than that corresponding to the distributions shown in figures 3 and 4 ($\overline{Re}_\infty = 6{\cdot}82$). In this instance the agreement between theory and experiment for $S = 3 \times 10^{-3}$ is not as good as that shown in figures 3 and 4. Kramers' correlation is apparently unable to describe precisely the local convective heat loss characteristics of a heated wire when a strong Reynolds number variation exists along its length. (For the conditions shown in figures 3 and 4, $\overline{Re}_\infty$ varies from 3·7 to 9·9, whereas, in figure 6, the variation is from 11·8 to 31·2.)

4.2. *Steady-state response behaviour*

For steady, uniform, isothermal mean flow over a heated wire at uniform temperature, the local Nusselt number is also uniform and, on the basis of (3), its functional dependency can be written as

$$Nu_f = Nu_f(Re_f, Pr_f, T_f/T_\infty). \tag{15}$$

If the wire is of finite length, however, and if a mean-velocity gradient exists along its length, then the local Nusselt number is no longer uniform. Furthermore, if d_s/d is relatively small, then $\overline{T}_s > T_\infty$, in general, and an end support temperature loading factor must be taken into account. Under these circumstances, it is expedient to define an overall Nusselt number for the wire, $\overline{Nu}_f$, whose functional dependency can be expressed as

$$\overline{Nu}_f = \overline{Nu}_f(\overline{Re}_f, \overline{Pr}_f, \overline{T}_f/T_\infty, \overline{T}_s/T_\infty, l/d, S). \tag{16}$$

An explicit form for $\overline{Nu}_f$ can be developed by integrating (1) over wire length to yield

$$\overline{Nu}_f = \frac{\overline{I}^2\overline{R}_{w,m} + a[k_{w,l}(d\overline{T}_w/dz)_l - k_{w,0}(d\overline{T}_w/dz)_0]}{\pi k_{f,m} l(\overline{T}_{w,m} - T_\infty)}. \tag{17}$$

If (17) were to be used to generate response curves interrelating $\overline{Nu}_f$ with the parameters of interest, then application of correction curves based on these plots would necessarily involve evaluation of the end conduction loss term in (17), i.e. $a[k_{w,l}(d\overline{T}_w/dz)_l - k_{w,0}(d\overline{T}_w/dz)_0]$. This is, of course, impractical in most situations, and therefore it is preferable to develop response curves referred to an overall wire Nusselt number which excludes end conduction losses, namely

$$\overline{Nu}'_f = \frac{\overline{I}^2\overline{R}_{w,m}}{\pi k_{f,m} l(\overline{T}_{w,m} - T_\infty)}. \tag{18}$$

Both $\overline{Nu}_f$ and $\overline{Nu}'_f$, however, are sensitive to $\overline{T}_s/T_\infty$, in general, and, before a final selection is made between the two Nusselt numbers, it is worthwhile to examine their relative dependency on $\overline{T}_s/T_\infty$. The computer program was used, therefore, to generate response curves of $\overline{Nu}_{f,\infty}/\overline{Nu}_f$ and $\overline{Nu}'_{f,\infty}/\overline{Nu}'_f$ as a function of $\overline{T}_s/T_\infty$ for typical operating conditions, where $\overline{Nu}_{f,\infty}$ and $\overline{Nu}'_{f,\infty}$ are evaluated at the condition $\overline{T}_s = T_\infty$.

Figure 7 shows the results of these computations. With reference to the figure, end support temperatures measured in the present study with $d_s/d \simeq 10$ correspond to $\overline{T}_s/T_\infty \simeq 1{\cdot}10$ and $1{\cdot}18$ for $\mathscr{H} = 0{\cdot}4$ and $0{\cdot}8$ respectively, and influence $\overline{Nu}'_f$ to the extent that $\overline{Nu}'_{f,\infty}/\overline{Nu}'_f \simeq 1{\cdot}025$ for both cases. For $d_s/d \simeq 20$, the measurements of Champagne (1966) indicate that $\overline{T}_s/T_\infty \simeq 1{\cdot}02$ and $1{\cdot}09$ for $\mathscr{H} = 0{\cdot}5$ and $0{\cdot}8$, respectively, over ranges $100 \leqslant l/d \leqslant 400$ and $8{\cdot}8 \leqslant \overline{Re}_\infty \leqslant 14{\cdot}5$. If his results are correlated with the results shown in figure 7, then

$$\overline{Nu}'_{f,\infty}/\overline{Nu}'_f \leqslant 1{\cdot}005,$$

provided $d_s/d \geqslant 20$. This implies that response curves based on Nu'_f are essentially independent of $\overline{T}_s/T_\infty$ over moderate ranges of $\overline{Re}_\infty$, l/d, and S whenever $d_s/d \geqslant 20$. This conclusion, coupled with the realization that correction curves referred to

$\overline{Nu'_f}$ can readily be applied in practice, prompted the selection of $\overline{Nu'_f}$ as the correlating Nusselt number. The results which follow were calculated for $\overline{T}_s/T_\infty = 1$ with $T_\infty = 20\,°\text{C}$, and are of general applicability as long as $d_s/d \geqslant 20$.

The influence of a mean-velocity gradient on the steady-state response characteristics of a hot wire is shown in figure 8 for typical operating conditions. The distributions for $S > 0$ exhibit rather remarkable behaviour in that $\overline{Nu'_f}$ varies linearly with $\overline{Re}_f^{\frac{1}{2}}$, even though both the local mean velocity across the

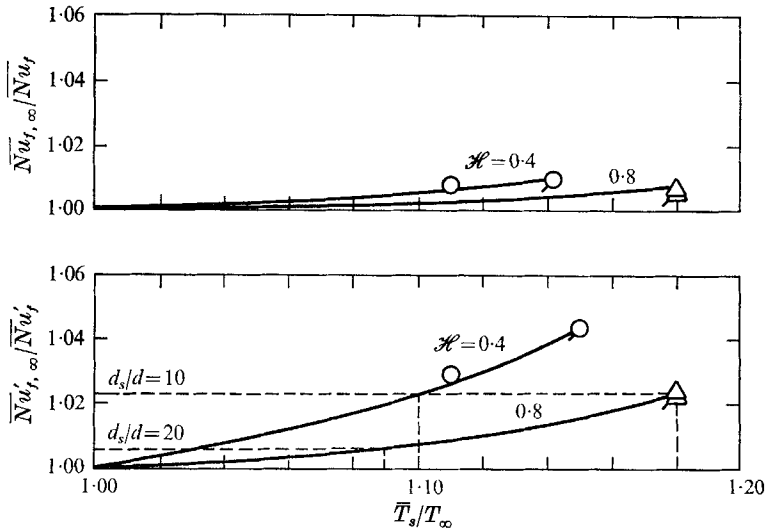

FIGURE 7. Effect of end support temperature variations on convective heat loss characteristics of platinum wires: $l/d = 300$, $\overline{Re}_\infty = 6{\cdot}82$, $T_\infty = 30\,°\text{C}$. Unflagged symbols, $S = 0$; flagged symbols, $S = 3 \times 10^{-3}$.

wire and local wire temperature are non-uniform. Computations of $\overline{Nu'_f}$ were performed at $\overline{Re}_\infty = 2{\cdot}14$, $13{\cdot}24$, $33{\cdot}82$, and $64{\cdot}00$ for both platinum and tungsten wires at $\mathscr{H} = 0{\cdot}4$ and $0{\cdot}8$. For all cases, the standard deviation of the slope $\Delta\overline{Nu'_f}/\Delta\overline{Re}_f^{\frac{1}{2}}$, as evaluated at each value of $\overline{Re}_\infty$, was less than $0{\cdot}012$. (Computer results for $\overline{Nu_f}$ indicated a slight, but consistent, decrease in values of the slope $\Delta\overline{Nu_f}/\Delta\overline{Re}_f^{\frac{1}{2}}$ with increasing values of $\overline{Re}_f^{\frac{1}{2}}$.)

The distributions in figure 8 show that the response of a hot wire becomes more sensitive to a mean-velocity gradient along its length as l/d increases. For a given l/d wire, response sensitivity to shear can be interpreted either as a displacement of the effective centre of the wire or as an influence on measurements at the actual wire centre. Displacement effect corrections could be generated from the results shown in figure 8, for example, by evaluating $\overline{Re}_{f,0}/\overline{Re}_f$ or, equivalently, $\overline{U}_{c,0}/\overline{U}_c$ at selected values of $\overline{Nu'_f}$. For a linear mean shear as shown in figure 1, $\overline{U}_{c,0}/\overline{U}_c$ can be related to a normalized displacement, $\Delta z/l$, as follows:

$$\Delta z/l = (d/Sl)\,(1 - \overline{U}_{c,0}/\overline{U}_c)$$

where Δz is the distance that the effective centre of the wire has been displaced in the direction of higher velocity.

For a given l/d wire, therefore, it is possible to replot results of the type shown in figure 8 as $\overline{Nu}'_f$ versus $\Delta z/l$ with $\Delta\overline{U}/\overline{U}_{c,0}$ as a parameter in place of S. In order to apply these normalized curves to a particular wire, it is necessary to transform values of $\overline{Nu}'_f$ to equivalent values of $\overline{E}$ for a particular set of operating conditions. If second-order temperature dependency effects are neglected, this procedure involves knowing ζ_1 in order to evaluate $\overline{T}_{w,m}-T_\infty$ in (18) from

$$\overline{T}_{w,m}-T_\infty = (\overline{R}_{w,m}-R_\infty)/\zeta_1 R_0,$$

where R_0 is the wire resistance at a reference temperature T_0. A problem exists, however, in specifying a value for ζ_1 because values of ζ_1 tabulated in the

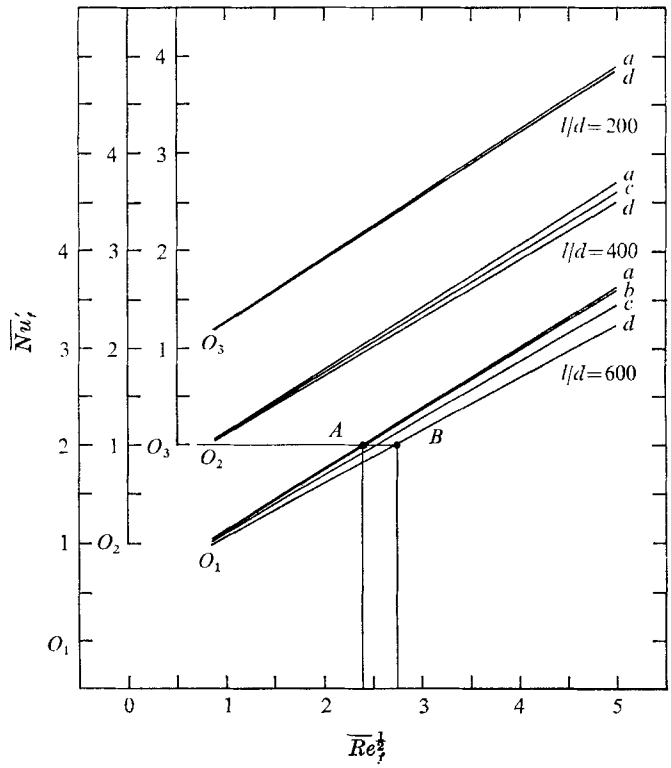

FIGURE 8. Influence of a mean-velocity gradient on steady-state response behaviour of platinum wires: $\mathscr{H} = 0{\cdot}8$. *a*, $S = 0$; *b*, $S = 1\times10^{-3}$; *c*, $S = 2\times10^{-3}$; *d*, $S = 3\times10^{-3}$.

literature for pure platinum and tungsten are not in close agreement for either material, and therefore a unique value of ζ_1 for each material cannot be specified from general reference data.

Because of the above-mentioned difficulties in specifying ζ_1, it is not possible to transform a set of normalized displacement effect correction curves to a set of working curves which apply universally for a given wire material. This problem can be circumvented, however, by treating response sensitivity to shear as an effect which influences measurements at the actual centre of a wire. This approach will therefore be adopted in interpreting the results of the present study. With

reference to figure 8 it can be seen that, if a mean velocity gradient exists along a wire, then application of the uniform flow calibration curve ($S = 0$) would underestimate the local mean velocity at the centre of the wire. As an example, consider a platinum wire with $l/d = 600$ to be located in a shear flow where $S = 3 \times 10^{-3}$. If the measurements yield a value $\overline{Nu}'_f = 2{\cdot}0$, then application of the $S = 0$ curve would predict a value $\overline{Re}_f^{\frac{1}{2}} = 2{\cdot}40$ (point A), whereas $\overline{Re}_f^{\frac{1}{2}}$ actually equals 2·75 (point B). This difference in values corresponds to underestimating the local mean velocity at the centre of the wire by approximately 24%.

The utilization of the response curves shown in figure 8 involves an iterative set of calculations because initially S is unknown and the uniform flow calibration curve must be used to estimate velocity profile configurations. Local values of S along a profile can then be evaluated, and reference made to a plot similar to figure 8 to correct the profile. The whole procedure must be repeated until successive velocity values converge to within specified limits.

The distributions shown in figure 8 are based on a particular set of reference data for platinum wire and, as such, are not directly applicable to platinum wires, in general, where thermophysical properties may vary from wire to wire. In order to develop correction curves of general applicability, the ratio $\overline{Nu}'_{f,0}/\overline{Nu}'_f$ was calculated as a function of $\overline{Re}_\infty$ where the subscript 0 denotes evaluation at uniform flow conditions. The results are shown in figures 9–10. These correction curves can be applied to any uniform flow calibration curve to construct a

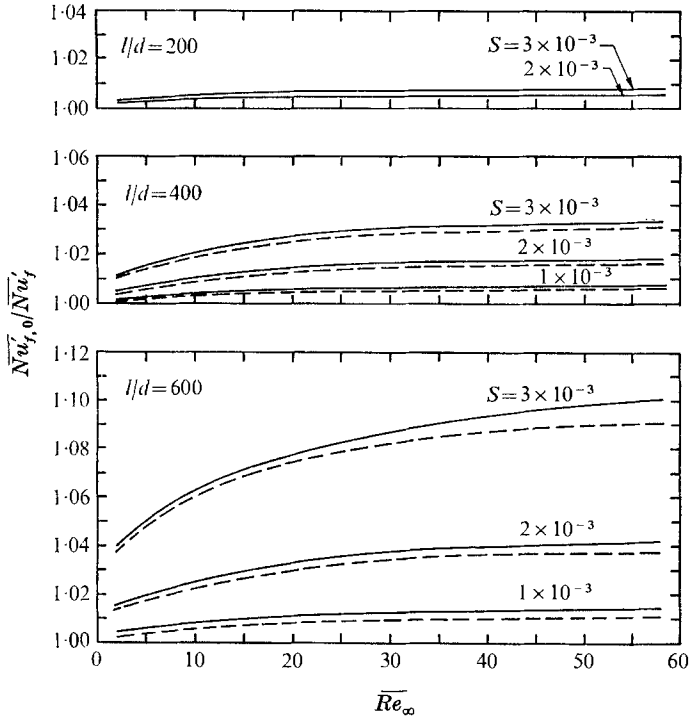

FIGURE 9. Steady-state response correction curves for platinum wires. ——, $\mathscr{H} = 0{\cdot}8$; – – –, $\mathscr{H} = 0{\cdot}4$.

family of curves of, say, $\overline{E}$ versus $\overline{U}_c$ for different values of S. The construction of a working plot in terms of quantities directly measurable on an anemometer is relatively simple because $\overline{Nu}'_{f,0}/\overline{Nu}'_f = (\overline{E}_0/\overline{E})^2 = (\overline{I}_0/\overline{I})^2$ for constant temperature operation at a fixed overheat ratio.

A comparison between figures 9 and 10 indicates that the steady-state response behaviour of tungsten wires is slightly less sensitive to shear than platinum wires for a given set of operating conditions. The figures also indicate that operation

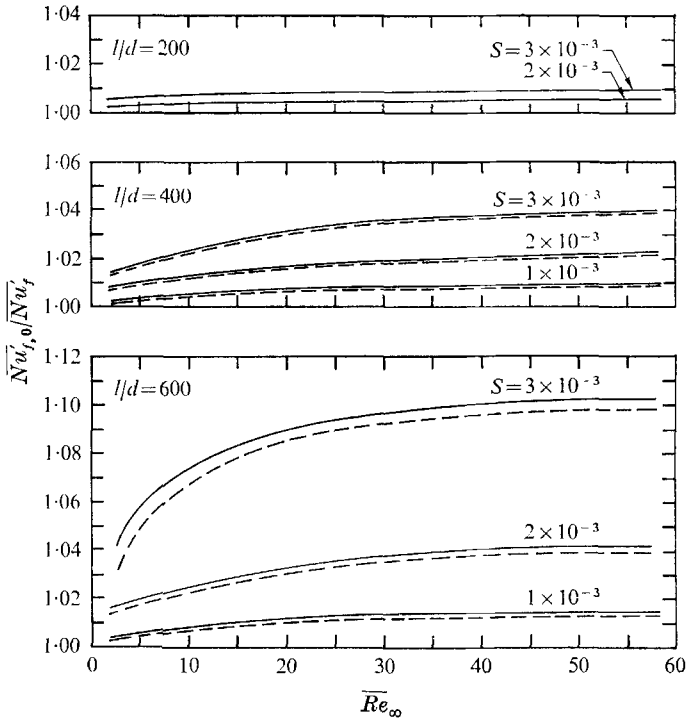

FIGURE 10. Steady-state response correction curves for tungsten wires. ——, $\mathscr{H} = 0{\cdot}8$; – – –, $\mathscr{H} = 0{\cdot}4$.

at $\mathscr{H} = 0{\cdot}4$ is preferable from the standpoint of minimizing shear flow sensitivity. Shear flow response is a relatively strong function of l/d, so that operation with minimum l/d wires is desirable, consistent, of course, with other requirements imposed by frequency response and probe design considerations.

4.3. *Dynamic response behaviour*

Results discussed in the previous section can be used to estimate the influence of a mean-velocity gradient on turbulence intensity measurements with a single wire normal to the flow. Figure 8, for example, shows that, when end conduction losses are excluded, steady-state response curves for $S \geqslant 0$ are of the form

$$\overline{Nu}'_f = A' + B'\overline{Re}_f^{\frac{1}{2}}, \tag{19}$$

where A' and B' denote the intercept at $\overline{Re}_f = 0$ and the slope, respectively, of each response curve. If a velocity fluctuation across a wire in a linear mean-velocity

gradient is idealized as being spatially uniform, then (18) and (19) can be applied at each instant of time. Since these equations are based on constant temperature operation, let $I = \bar{I} + i'$, $U_c = \bar{U}_c + u'$, $\bar{R}_w \simeq \bar{R}_{w,m}$, $\bar{T}_w \simeq \bar{T}_{w,m}$ and note that $e' = \bar{R}_{w,m} i' \equiv su'$, where e' is a voltage fluctuation and s is the wire sensitivity. Assume now small velocity fluctuations so that second-order effects can be neglected; then

$$s = \frac{\pi k_{f,m} l(\bar{T}_{w,m} - T_\infty)}{4\bar{I}} \left(\frac{d}{\bar{U}_c \nu_{f,m}}\right) B'. \tag{20}$$

If a heated wire is operated at constant temperature in a shear flow of unknown characteristics it will yield a mean output ($\bar{E}$ or $\bar{I}$) whose correlation with the local mean velocity will initially be unknown. If reference is made to a uniform flow calibration curve without performing any corrections, then, on the basis of results shown in figure 8, $\bar{U}_c$ and B' in (20) will be underestimated and overestimated, respectively. The influence that this has on wire sensitivity can be estimated by examining the behaviour of s_0/s over a range of operating conditions, where s_0 is the uniform flow wire sensitivity. For a given mean wire output corresponding to a fixed set of operating conditions, it follows that

$$\frac{s_0}{s} = \frac{B'_0}{B'} \left(\frac{\bar{U}_c}{\bar{U}_{c,0}}\right)^{\frac{1}{2}}. \tag{21}$$

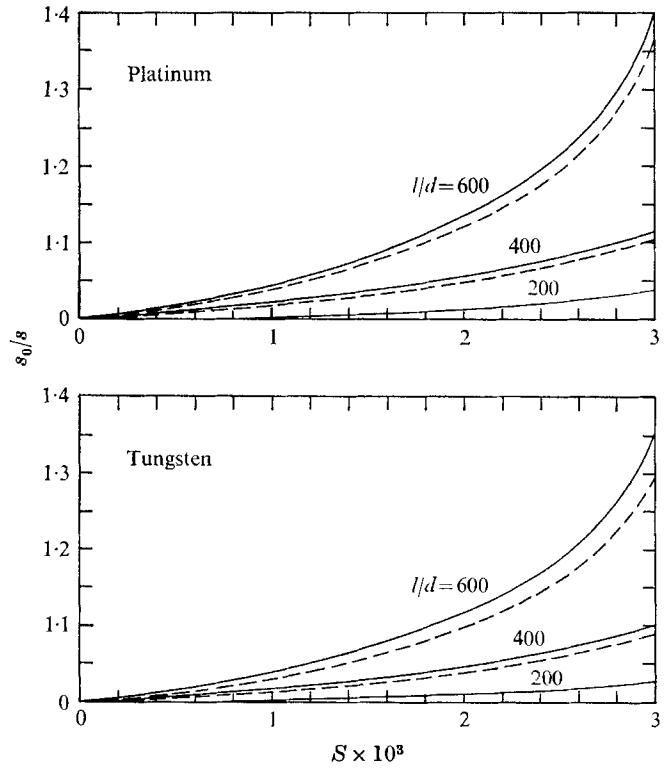

FIGURE 11. Influence of a mean-velocity gradient on the sensitivity of platinum and tungsten wires to velocity fluctuations. ——, $\mathscr{H} = 0{\cdot}8$; – – –, $\mathscr{H} = 0{\cdot}4$.

The behaviour of s_0/s over a range of operating conditions is shown in figure 11. The distributions are universal functions over the Reynolds number range of the calculations ($2{\cdot}14 \leqslant \overline{Re}_\infty \leqslant 64$) and indicate that wire sensitivity to fluctuations is diminished when shearing effects are present. Since $e' = su'$, it also follows that, for a given r.m.s. output voltage, $\tilde{u}'/\tilde{u}'_0 = s_0/s$, where $\tilde{u}'_0$ is the apparent turbulence intensity calculated from the uniform flow wire sensitivity and $\tilde{u}'$ is the actual intensity. Since $s_0/s > 1$ whenever $S > 0$, $\tilde{u}'_0$ will underestimate the actual intensity whenever a hot wire is exposed to a mean-velocity gradient. If turbulence intensity measurements are to be made with a wire which cannot be oriented to eliminate a gradient along its length, then the mean-velocity profile should first be corrected in order to determine $\overline{U}_c$ and S at each measuring point and, in turn, B' from the calibration plot. The turbulence intensity may then be calculated from the measured r.m.s. voltage output, $\tilde{e}'$, and s, as evaluated from (20) or, alternatively, from figure 11 after $\tilde{u}'_0$ has been evaluated.

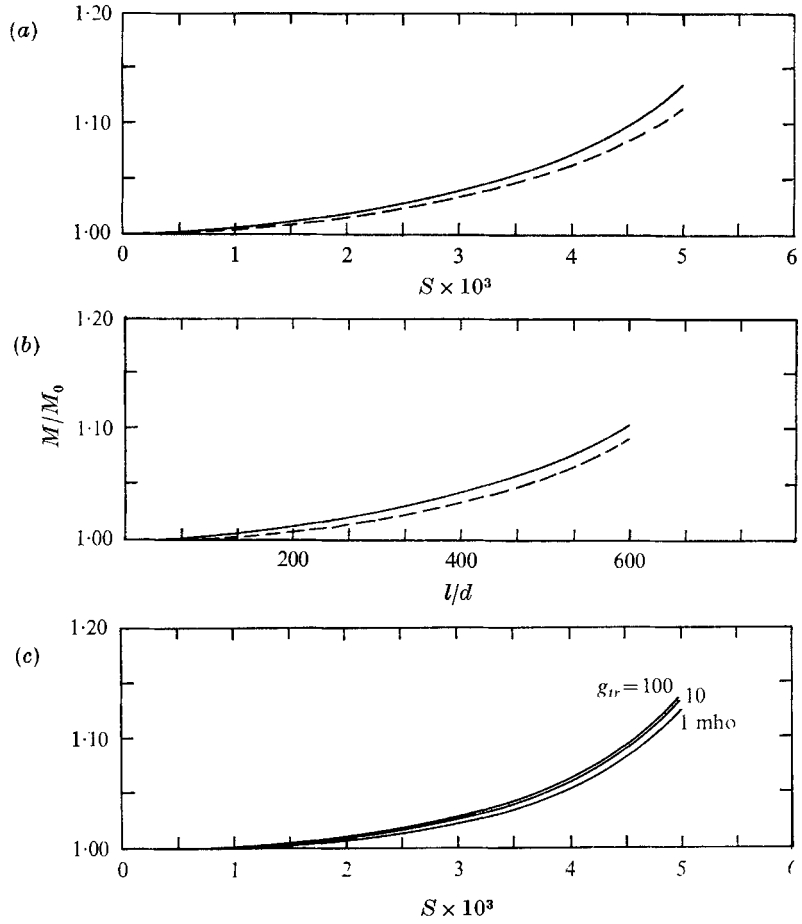

FIGURE 12. Influence of a mean-velocity gradient on the time constant behaviour of platinum and tungsten wires: $\overline{Re}_\infty = 33{\cdot}8$. (*a*) $l/d = 400$; $g_{tr} = 10$ mhos, $0{\cdot}4 \leqslant \mathscr{H} \leqslant 0{\cdot}8$. (*b*) $S = 3 \times 10^{-3}$, $g_{tr} = 10$ mhos, $0{\cdot}4 \leqslant \mathscr{H} \leqslant 0{\cdot}8$. (*c*) $l/d = 400$, $\mathscr{H} = 0{\cdot}8$. ——, platinum; – – –, tungsten.

As discussed earlier, the time constant of a hot-wire probe–anemometer system is influenced by the presence of a mean-velocity gradient along the wire. Results from the computer program were used in conjunction with (14) to generate response curves for M/M_0 where M_0 is the time constant evaluated at uniform flow conditions. The results of these computations are shown in figure 12, where the trends exhibited by the distributions should be regarded as qualitative rather than quantitative because of the rather limiting assumptions made in the development of (14). For a given l/d wire and transconductance of the amplifier circuit, the upper figure shows that M/M_0 increases as S increases, with tungsten wire being slightly less shear sensitive in comparison to platinum wire. For a given mean-velocity gradient the middle figure indicates that M/M_0 also increases as l/d increases. The gradient response of M/M_0 is relatively insensitive to g_{tr}, as indicated by the lower figure, so selection of an operating value of g_{tr} can be made independent of gradient considerations. For all cases examined herein, $M/M_0 < 1{\cdot}10$ as long as $l/d < 600$ and $S < 3 \times 10^{-3}$. Since these limiting values represent rather extreme conditions, it appears that the selection of a wire exposed to a mean shear can be made on the basis of its time constant characteristics for $S = 0$, as long as a possible 10% increase in M can be tolerated.

5. Conclusions

The presence of a mean-velocity gradient along the length of a hot wire operated at constant temperature causes a skewed wire temperature distribution which influences both the steady-state and dynamic response characteristics of the wire. If a uniform flow calibration curve is used to evaluate the local mean velocity at the centre of a wire exposed to a mean shear, the value will be underestimated whenever $S > 0$. The presence of a mean shear across a wire will also cause a decrease in its sensitivity to velocity fluctuations. If the uniform flow wire sensitivity is used to evaluate the turbulence intensity at the centre of a wire, then, for a given r.m.s. voltage output, the value will be underestimated whenever $S > 0$. The influence of S on both steady-state and dynamic response behaviour increases as l/d increases for otherwise fixed operating conditions. From the standpoint of minimum shear sensitivity, therefore, consistent with other considerations, wires with $l/d \sim O(200)$ are recommended. Response sensitivity to shear increases slightly with an increase in overheat ratio in the range $0{\cdot}4 \leqslant \mathscr{H} \leqslant 0{\cdot}8$, with tungsten wire being slightly less shear sensitive than platinum wire over the range of variables considered in the present work.

In order to draw still more specific conclusions about upper limits for corrections under typical operating conditions, consider the following: Assume that a 5μ platinum wire with $l/d = 400$ is located in air flow where $10 \leqslant \overline{U}_c \leqslant 100$ m/sec and $T_\infty = 20$ °C ($3{\cdot}3 \leqslant \overline{Re}_\infty \leqslant 33$). If the wire is operated at $\mathscr{H} = 0{\cdot}8$ in shear flow where $S = 2 \times 10^{-3}$, then $\overline{U}_c$ will be underestimated by a maximum of 4·3% if the uniform flow calibration curve is used. If l/d is decreased to 200, then, over the same range of operating conditions, this percentage difference will decrease to 1·3%. Over the Reynolds number range of the calculations ($2{\cdot}14 \leqslant \overline{Re}_\infty \leqslant 64$), $\tilde{u}'_0$ calculated from the uniform flow wire sensitivity will

underestimate $\tilde{u}'$ by a maximum of 5·8 % for an $l/d = 400$ wire and the operating conditions cited above. If $l/d = 200$, this percentage difference decreases to 1·4 %. For tungsten wires and lower overheat ratios, the above-mentioned percentage differences are even less. Under typical operating conditions, therefore, shear flow corrections will be on the order of only 1 % or less, provided $l/d \leqslant 200$ and $S \leqslant 2 \times 10^{-3}$. For applications where larger l/d wires must be used, shear flow corrections can become important, however, especially if a wire is exposed to a highly sheared mean flow along its length.

This study was made possible by financial support from the Graduate School Research Fund and the Office of Engineering Research at the University of Washington. The authors would like to thank Professor Ashley F. Emery for his help with the computer programming. The authors would also like to express their gratitude to the Barnes Engineering Company for the use of one of the RM-2A infrared microscopes for the temperature distribution measurements discussed herein.

REFERENCES

CHAMPAGNE, F. H. 1966 Turbulence measurements with inclined wires. Ph.D. Thesis, University of Washington.

CHAMPAGNE, F. H., SLEICHER, C. A. & WEHRMANN, O. H. 1967 Turbulence measurements with inclined hot-wires. Part 1. Heat transfer experiments with inclined hot-wire. *J. Fluid Mech.* **28**, 153.

COLLIS, D. C. & WILLIAMS, M. J. 1959 Two-dimensional convection from heated wires at low Reynolds numbers. *J. Fluid Mech.* **6**, 357.

CORRSIN, S. 1963 Turbulence: Experimental methods. *Handbuch der Physik*, 1st ed., vol. VIII/2, 525. Berlin: Springer-Verlag.

DAVIES, P. O. A. L. & BRUUN, H. H. 1968 The performance of a yawed hot wire. *Proc. of a Symp. on Instr. and Data Proc. for Ind. Aero.*, 10.1. National Physical Laboratory, Teddington (England).

DAVIES, P. O. A. L. & FISHER, M. J. 1964 Heat transfer from electrically heated cylinders. *Proc. Roy. Soc.* A **280**, 486.

FRIEHE, C. A. & SCHWARZ, W. H. 1968 Deviations from the cosine law for yawed cylindrical anemometer sensors. *Trans. of ASME, J. Appl. Mech.* **35**, 655.

FURTH, W. F. 1956 Hot-wire response to a parabolic velocity. M.S. Thesis, Johns Hopkins University.

HINZE, J. O. 1959 *Turbulence*, 1st ed. New York: McGraw-Hill.

KJELLSTRÖM, B. & HEDBERG, S. 1968 Turbulence and shear stress measurements in a circular channel for testing of hot-wire anemometer measurement techniques and evaluation methods. *A.B. Atomenergi* RTL-1001 (Sweden).

KRAMERS, H. 1946 Heat transfer from spheres to flowing media. *Physica*, **12**, 61.

MATTIOLI, E. 1956 Una nuova sonda a filo caldo per misure di turbolenza nello strato limite. *Atti della Accademia delle Scienze di Torino, I. Classe di Scienze Fisiche, Matematiche e. Naturali*, **91**, 71.

MOLLER, G. L. 1969 Measurement of mean-flow velocity in shear flow. M.S. Thesis, University of Washington.

VAN DER HEGGE ZIJNEN, B. G. 1956 Modified correlation formulae for the heat transfers by natural and by forced convection from horizontal cylinders. *Appl. Sci. Res.* A **6**, 129.